Supplementary Material

Donnan Dialysis for Phosphate Recovery from Diverted Urine

Water Research

Stephanie N. McCartney[a], Hanqing Fan[a], Nobuyo Watanabe[b], Yuxuan Huang[a], and Ngai Yin Yip[*a,c]

[a] Department of Earth and Environmental Engineering, Columbia University, New York, New York 10027-6623, United States

[b] Department of Chemistry, Barnard College, New York, New York 10027-6598, United States

[c] Columbia Water Center, Columbia University, New York, New York 10027-6623, United States

DONNAN EQUILIBRIUM

Binary Systems. At Donnan equilibrium, the electrochemical potentials of a charged species, *i*, in the feed solution, FS, and receiver solution, RS, are equal, as described by eq S1.

$$\mu_i^0 + RT \ln a_{i,\mathrm{RS},f} + z_i F \psi_{\mathrm{RS},f} = \mu_i^0 + RT \ln a_{i,\mathrm{FS},f} + z_i F \psi_{\mathrm{FS},f} \tag{S1}$$

where μ is chemical potential, T is absolute temperature, a is activity, z is ion valence, ψ is electrical potential, R is the gas constant, and F is Faraday's constant; superscript 0 indicates standard state, whereas subscripts f, FS, and RS refer to final state, feed stream, and receiver stream, respectively. Rearranging eq S1 yields:

$$\frac{F\left(\psi_{\mathrm{RS},f} - \psi_{\mathrm{FS},f}\right)}{RT} = \ln\left(\frac{a_{i,\mathrm{FS},f}}{a_{i,\mathrm{RS},f}}\right)^{1/z} \tag{S2}$$

In Donnan dialysis, DD, with initial conditions of $H_xPO_4^{(3-x)-}$ as the sole anion in the FS and Cl^- as the sole anion in the RS, the final activities of $H_xPO_4^{(3-x)-}$ and Cl^- in the FS and RS are related to the electrical potential between the FS and RS, $\Psi_{\mathrm{RS},f} - \Psi_{\mathrm{FS},f}$:

$$\frac{F\left(\psi_{\mathrm{RS},f} - \psi_{\mathrm{FS},f}\right)}{RT} = \ln\left(\frac{a_{\mathrm{H_xPO_4}^{(3-x)-},\mathrm{FS},f}}{a_{\mathrm{H_xPO_4}^{(3-x)-},\mathrm{RS},f}}\right)^{1/(3-x)} \tag{S3}$$

$$\frac{F\left(\psi_{\mathrm{RS},f} - \psi_{\mathrm{FS},f}\right)}{RT} = \ln\left(\frac{a_{\mathrm{Cl^-},\mathrm{FS},f}}{a_{\mathrm{Cl^-},\mathrm{FS},f}}\right) \tag{S4}$$

Because $\Psi_{\mathrm{RS},f} - \Psi_{\mathrm{FS},f}$ is the same for the two ions, eqs S3 and S4 can be combined. Further assuming activity coefficients, γ, approximate to unity simplifies activities to molar concentrations: $a = \gamma[i] \approx [i]$, yielding eq 1 in the main manuscript.

$$\frac{\left[\mathrm{H_xPO_4}^{(3-x)-}\right]_{\mathrm{FS},f}}{\left[\mathrm{H_xPO_4}^{(3-x)-}\right]_{\mathrm{RS},f}} \approx \left(\frac{\left[\mathrm{Cl^-}\right]_{\mathrm{FS},f}}{\left[\mathrm{Cl^-}\right]_{\mathrm{RS},f}}\right)^{(3-x)} \tag{1}$$

The final concentrations at Donnan equilibrium can be determined by applying material balance using initial $H_xPO_4^{(3-x)-}$ and Cl^- concentrations, represented by subscript 0. To maintain electroneutrality, one $H_xPO_4^{(3-x)-}$ ion exchanges with $(3-x)Cl^-$ ion(s) across the anion exchange

membrane. As $\left[\mathrm{H_xPO_4^{(3-x)-}}\right]_{\mathrm{RS},0} = 0$ and $\left[\mathrm{Cl^-}\right]_{\mathrm{FS},0} = 0$, and for specific scenario of equal RS and FS volumes, i.e., $V_{\mathrm{RS}} = V_{\mathrm{FS}}$, eqs S6–7 are material balances for the ions.

$$\left[\mathrm{H_xPO_4^{(3-x)-}}\right]_{\mathrm{RS},f} = (3-x)\left[\mathrm{Cl^-}\right]_{\mathrm{FS},f} \tag{S5}$$

$$\left[\mathrm{H_xPO_4^{(3-x)-}}\right]_{\mathrm{FS},f} = \left[\mathrm{H_xPO_4^{(3-x)-}}\right]_{\mathrm{FS},0} - \left[\mathrm{H_xPO_4^{(3-x)-}}\right]_{\mathrm{RS},f} \tag{S6}$$

$$\left[\mathrm{Cl^-}\right]_{\mathrm{FS},f} = \left[\mathrm{Cl^-}\right]_{\mathrm{RS},0} - \left[\mathrm{Cl^-}\right]_{\mathrm{RS},f} \tag{S7}$$

Substituting eqs S6 and S7 into eq 1 yields eq S8.

$$\frac{\left[\mathrm{H_xPO_4^{(3-x)-}}\right]_{\mathrm{FS},0} - \left[\mathrm{H_xPO_4^{(3-x)-}}\right]_{\mathrm{RS},f}}{\left[\mathrm{H_xPO_4^{(3-x)-}}\right]_{\mathrm{RS},f}} \approx \left(\frac{(3-x)\left[\mathrm{H_xPO_4^{(3-x)-}}\right]_{\mathrm{RS},f}}{\left[\mathrm{Cl^-}\right]_{\mathrm{RS},0} - (3-x)\left[\mathrm{H_xPO_4^{(3-x)-}}\right]_{\mathrm{RS},f}}\right)^{(3-x)} \tag{S8}$$

Therefore, final concentrations of $H_xPO_4^{(3-x)-}$ and Cl^- in the FS and RS at Donnan equilibrium can be determined using the initial concentrations.

Multi-Component Systems. Following the same approach presented above, the following Donnan equilibrium expression can be derived for DD with the initial FS containing multiple anions of $H_xPO_4^{(3-x)-}$, SO_4^{2-}, and Cl^- by substituting the anions for *i*.

$$\left(\frac{\left[\mathrm{H_xPO_4^{(3-x)-}}\right]_{\mathrm{FS}}}{\left[\mathrm{H_xPO_4^{(3-x)-}}\right]_{\mathrm{RS}}}\right)^{1/(3-x)} \approx \left(\frac{\left[\mathrm{Cl^-}\right]_{\mathrm{FS}}}{\left[\mathrm{Cl^-}\right]_{\mathrm{RS}}}\right) = \left(\frac{\left[\mathrm{SO_4^{2-}}\right]_{\mathrm{FS}}}{\left[\mathrm{SO_4^{2-}}\right]_{\mathrm{RS}}}\right)^{1/2} \tag{S9}$$

Similarly, initial concentrations of $H_xPO_4^{(3-x)-}$, SO_4^{2-}, and Cl^- in the FS and RS can be utilized to determine final ion concentrations at Donnan equilibrium. The following presentation considers equivalent RS and FS volumes. To maintain electroneutrality, Cl^- transport from the RS to FS is balanced by $H_xPO_4^{(3-x)-}$ and SO_4^{2-} transport from the FS to RS, as described in eq S10. Eqs S11–13 are material balances for each ion.

$$\left[\mathrm{Cl^-}\right]_{\mathrm{FS},f} = (3-x)\left[\mathrm{H_xPO_4^{(3-x)-}}\right]_{\mathrm{RS},f} + 2\left[\mathrm{SO_4^{2-}}\right]_{\mathrm{RS},f} + \left[\mathrm{Cl^-}\right]_{\mathrm{FS},0} \tag{S10}$$

$$\left[\mathrm{H_xPO_4^{(3-x)-}}\right]_{\mathrm{FS},f} = \left[\mathrm{H_xPO_4^{(3-x)-}}\right]_{\mathrm{FS},0} - \left[\mathrm{H_xPO_4^{(3-x)-}}\right]_{\mathrm{RS},f} \tag{S11}$$

$$\left[\mathrm{SO_4^{2-}}\right]_{\mathrm{FS},f} = \left[\mathrm{SO_4^{2-}}\right]_{\mathrm{FS},0} - \left[\mathrm{SO_4^{2-}}\right]_{\mathrm{RS},f} \tag{S12}$$

$$\left[\mathrm{Cl^-}\right]_{\mathrm{FS},f} = \left[\mathrm{Cl^-}\right]_{\mathrm{FS},0} + \left[\mathrm{Cl^-}\right]_{\mathrm{RS},0} - \left[\mathrm{Cl^-}\right]_{\mathrm{RS},f} \tag{S13}$$

Solving eqs S9–13 gives the final concentrations of $H_xPO_4^{(3-x)-}$, SO_4^{2-}, and Cl^- in the FS and RS.

Systems with Different FS and RS Volumes. In the systems presented earlier, the FS and RS volumes are equal. In systems where $V_{\mathrm{FS}} \neq V_{\mathrm{RS}}$, $[i]_{\mathrm{FS},0} - [i]_{\mathrm{FS},f} \neq [i]_{\mathrm{RS},f} - [i]_{\mathrm{RS},0}$ because of the differences in FS and RS volumes. Factoring in the FS and RS volumes, Cl^- transport from the RS to FS is balanced by $H_xPO_4^{(3-x)-}$ and SO_4^{2-} transport from the FS to RS:

$$\left[\mathrm{Cl^-}\right]_{\mathrm{FS},f} V_{\mathrm{FS}} = (3-x)\left[\mathrm{H_xPO_4^{(3-x)-}}\right]_{\mathrm{RS},f} V_{\mathrm{RS}} + 2\left[\mathrm{SO_4^{2-}}\right]_{\mathrm{RS},f} V_{\mathrm{RS}} + \left[\mathrm{Cl^-}\right]_{\mathrm{FS},0} V_{\mathrm{FS}} \tag{S14}$$

The following material balances for the multi-component system, eq S15–17, account for different FS and RS volumes. Again, knowing the initial ion concentrations enables the final ion concentrations in the FS and RS at Donnan equilibrium to be determined.

$$\left[\mathrm{H_xPO_4^{(3-x)-}}\right]_{\mathrm{FS},f} V_{\mathrm{FS}} = \left[\mathrm{H_xPO_4^{(3-x)-}}\right]_{\mathrm{FS},0} V_{\mathrm{FS}} - \left[\mathrm{H_xPO_4^{(3-x)-}}\right]_{\mathrm{RS},f} V_{\mathrm{RS}} \tag{S15}$$

$$\left[\mathrm{SO_4^{2-}}\right]_{\mathrm{FS},f} V_{\mathrm{FS}} = \left[\mathrm{SO_4^{2-}}\right]_{\mathrm{FS},0} V_{\mathrm{FS}} - \left[\mathrm{SO_4^{2-}}\right]_{\mathrm{RS},f} V_{\mathrm{RS}} \tag{S16}$$

$$\left[\mathrm{Cl^-}\right]_{\mathrm{FS},f} V_{\mathrm{FS}} = \left[\mathrm{Cl^-}\right]_{\mathrm{FS},0} V_{\mathrm{FS}} + \left[\mathrm{Cl^-}\right]_{\mathrm{RS},0} V_{\mathrm{RS}} - \left[\mathrm{Cl^-}\right]_{\mathrm{RS},f} V_{\mathrm{RS}} \tag{S17}$$

SIMULATED WASTE WATER SOFTENING REGENERANT RINSE

Water softening systems typically utilize salts with a monovalent cation (generally NaCl or KCl) to exchange with the captured polyvalent cations (primarily Ca^{2+} and Mg^{2+}) in the regeneration process. The regenerant salts are supplied well in excess of stoichiometry and, thus, the recharge wastewaters, termed waste water softening regenerant rinse, have high concentrations of Cl^- (as either NaCl or KCl). A solution of mainly $KCl_{(aq)}$ was prepared to simulate the waste water softening regenerant rinse, for use as the receiver solution in DD recovery of orthophosphate. Using the specifications of commercially available water softening products from PuroLite(2021) (Table S1) and material flow of the water softening system (calculated values shown in Table S2), the composition of typical waste water softening regenerant rinse was determined (Table S3). Note that hardness was simulated with $MgCl_2$ (i.e., no Ca^{2+}).

Table S1. Specifications for commercially available water softening products from PuroLite (2021).

Specification	Value
Maximum theoretical capacity for KCl (grains/lb-KCl)(Michaud, 1999a; b)	4,708
Typical Capacity, 65% Max (grains/lb-KCl)(Michaud, 1999a; b)	2,660
Typical Dose of KCl (lb/ft^3 resin)(2021)	20
Volume of resin (ft^3)(2021)	1
Drain for regeneration, i.e., water volume added to flush (L/ft^3 resin)(2021)	189

Table S2. Calculated values based on material flow using the specifications in Table 1.

Calculation	Value
Typical Dose (Moles of KCl)	122
Typical Capacity (Moles of Ca^{2+} and Mg^{2+}/lb resin)	0.45
Divalent Cations (M^{2+}) Released in Waste stream (Moles of Ca^{2+} and Mg^{2+})	9.09
K^+ Ions Remaining (Moles)	103
Cl^- Ions (Moles)	122

Table S3. Composition of a typical waste water softening regenerant rinse, determined using the specifications in Table 1 and calculated values in Table 2.

Species	Concentration ($\times 10^{-3}$ mol/L)
KCl	547
$MgCl_2$	48
Total Cl^-	644

SIMULATED DILUTED BITTERN

Bittern brine is the liquid stream that remains after the crystallization of table salt from seawater. The composition of bittern brine is shown in Table S4. Note that bittern brine is highly concentrated in chloride at 6.15 mol/L. To achieve a $[Cl^-] \approx 600 \times 10^{-3}$ mol/L, a dilution factor of 10 was utilized, and the composition of the diluted stream is presented in Table S4. The diluted bittern solution utilized in DD experiments (252×10^{-3} mol/L $MgCl_2 \cdot 6H_2O$, 77×10^{-3} mol/L KCl, 25×10^{-3} mol/L $MgSO_4 \cdot 7H_2O$, 26×10^{-3} mol/L NaCl, and 8×10^{-3} mol/L NH_4Cl) accounts for all major ions (excluding Ca^{2+} and Br^-).

Table S4. Typical ion concentrations in bittern brine(Kuda and Yano, 2014) and bittern brine diluted by a factor of 10.

	Bittern Brine (mol/L)	**Bittern Brine Diluted by a Factor of 10 ($\times 10^{-3}$ mol/L)**
Na^+	0.26	26
NH_4^+	0.08	8
K^+	0.14	14
Mg^{2+}	2.77	277
Ca^{2+}	trace	trace
Cl^-	6.15	615
Br^-	trace	trace
SO_4^{2-}	0.25	25

Table S5. Summary of conditions for experiments presented in Figures 2−8 of the main manuscript.

Figure	**Feed Solution (FS)**	**Receiver Solution (RS)**	**V_{RS}/V_{FS}**	**Membrane**	**Experiment Type**
2	Constant: 30 $\times 10^{-3}$ mol/L TOP	Constant: 600 $\times 10^{-3}$ mol/L NaCl	Constant: 1	Constant: Selemion AMV	N/A
3	Constant: 30 $\times 10^{-3}$ mol/L TOP	Varied [Cl^-]	Constant: 1	Constant: Selemion AMV	Equilibrium
4	Constant: 30 $\times 10^{-3}$ mol/L TOP	Constant: 600 $\times 10^{-3}$ mol/L NaCl	Varied: 1, 2, 4	Constant: Selemion AMV	Equilibrium
5	Varied	Constant: 600 $\times 10^{-3}$ mol/L NaCl	Constant: 2	Constant: Selemion AMV	Equilibrium
6	Varied	Constant: 600 $\times 10^{-3}$ mol/L NaCl	Constant: 1	Constant: Selemion AMV	Kinetic
7	Constant: simulated fresh urine	Constant: 600 $\times 10^{-3}$ mol/L NaCl	Constant: 1	Varied: Selemion AMV and Selemion ASVN	Kinetic
8	Constant: simulated fresh urine	Varied	Constant: 1	Constant: Selemion AMV	Kinetic

EFFECTS OF COMPETING ANIONS ON RECOVERY

To uncouple the relative impact of the three factors of i) competition with SO_4^{2-} ions, ii) competition with HCO_3^- ions, and iii) the weakened driving force due to Cl^- ions in the FS on orthophosphate recovery, theoretical $[H_xPO_4^{(3-x)-}]_{RS,f}$ were calculated for DD with FS containing i) $H_xPO_4^{(3-x)-}$ and SO_4^{2-}, ii) $H_xPO_4^{(3-x)-}$ and HCO_3^-, and iii) $H_xPO_4^{(3-x)-}$ and Cl^-. These calculated values are presented in Figure S1, together with the theoretical $[H_xPO_4^{(3-x)-}]_{RS,f}$ with FS of TOP-only, fresh urine, and hydrolyzed urine. When included in the FS, $H_xPO_4^{(3-x)-}$, SO_4^{2-}, Cl^-, and HCO_3^- ion concentrations are 30 $\times 10^{-3}$, 16 $\times 10^{-3}$, 100 $\times 10^{-3}$, and 250 $\times 10^{-3}$ mol/L, respectively. Inclusion of Cl^- ions to the feed matrix lowers $[H_xPO_4^{(3-x)-}]_{RS,f}$ by more than 2× compared to the inclusion of SO_4^{2-} (23.3% and 10.4% reductions for iii and i, respectively, relative to TOP-only feed solution). Therefore, the decrease in Cl^- concentration gradient driving force impacts orthophosphate recovery more than the competition posed by SO_4^{2-} ions in urine. The introduction of HCO_3^- ions, as in hydrolyzed urine, substantially lowers $[H_xPO_4^{(3-x)-}]_{RS,f}$ by 32.0% compared with the TOP-only FS, which is even larger than the 30.3% reduction observed with the combined inclusion of SO_4^{2-} and Cl^- ions, i.e., fresh urine. Therefore, the competition posed by HCO_3^- in hydrolyzed urine is the main reason projected $[H_xPO_4^{(3-x)-}]_{RS,f}$ is significantly lower than in DD with TOP-only FS.

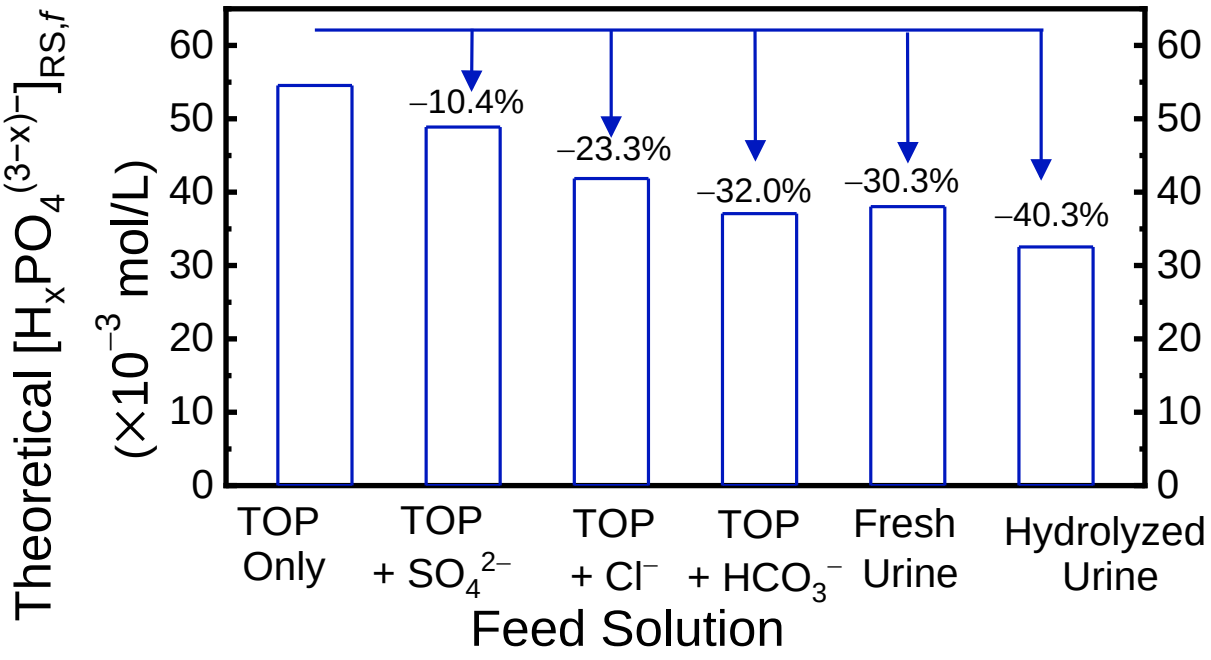

Figure S1. Theoretical $[H_xPO_4^{(3-x)-}]_{RS,f}$ in DD operation with FS containing different anions. If present in the FS, $H_xPO_4^{(3-x)-}$, SO_4^{2-}, Cl^-, and HCO_3^- ion concentrations are 30×10^{-3} mol/L, 16×10^{-3} mol/L, 100×10^{-3} mol/L, and 250×10^{-3} mol/L, respectively. The decreases in $[H_xPO_4^{(3-x)-}]_{RS,f}$ relative to the FS containing $H_xPO_4^{(3-x)-}$ only are displayed as labels above the columns. V_{FS}/V_{RS} equal to 2 and receiver solution is 600×10^{-3} mol/L NaCl.

IMPACT OF REDUCED DRIVING FORCE ON ORTHOPHOSPHATE FLUX

The inclusion of anions other than $H_xPO_4^{(3-x)-}$ in the feed solution lowers the orthophosphate that can be theoretically recovered in DD (Figure 5A of the main manuscript) by reducing the driving force for $H_xPO_4^{(3-x)-}$ transport. To quantitatively explore the impact of the reduced driving force on $H_xPO_4^{(3-x)-}$ fluxes, J_P, we examine $\Delta[H_xPO_4^{(3-x)-}] \equiv [H_xPO_4^{(3-x)-}]_{FS,0} - [H_xPO_4^{(3-x)-}]_{FS,f}$, defined as the difference between initial and final (at Donnan equilibrium) TOP concentrations in the feed solution. $\Delta[H_xPO_4^{(3-x)-}]$ can be intuitively understood as the equivalent amount of ions that should be transported to the RS in Donnan dialysis. Table S6 displays $\Delta[H_xPO_4^{(3-x)-}]$ and the percentage decrease in $\Delta[H_xPO_4^{(3-x)-}]$ relative to DD with $H_xPO_4^{(3-x)-}$-only FS for different ions in the feed solution. The inclusion of SO_4^{2-} and Cl^- lower $\Delta[H_xPO_4^{(3-x)-}]$ by 5.26% and 13.7%, respectively, while having both ions decreases the driving force by 18.0%. However, the reductions in J_P with additional ions in the FS are drastically more pronounced (60–90%) than reductions in $\Delta[H_xPO_4^{(3-x)-}]$ (5.3–18%). Importantly, normalizing the ion fluxes of Figure 6 of the main manuscript by $\Delta[H_xPO_4^{(3-x)-}]$ gave vastly dissimilar values for the different FS anion compositions (Figure S2), providing strong evidence that the lessened $\Delta[H_xPO_4^{(3-x)-}]$ does not fully explain the diminished J_P.

Table S6. $\Delta[H_xPO_4^{(3-x)-}]$ in the feed solution, in operation with FS containing different anions. $\Delta[H_xPO_4^{(3-x)-}] \equiv [H_xPO_4^{(3-x)-}]_{FS,0} - [H_xPO_4^{(3-x)-}]_{FS,f}$ is defined as the difference between initial and final (at Donnan equilibrium) total orthophosphate concentrations in the feed solution. If present in the FS, $H_xPO_4^{(3-x)-}$, SO_4^{2-}, Cl^-, and HCO_3^- ion concentrations are 30×10^{-3} mol/L, 16×10^{-3} mol/L, 100×10^{-3} mol/L, and 250×10^{-3} mol/L, respectively. The decrease in $\Delta[H_xPO_4^{(3-x)-}]$ relative to the FS containing $H_xPO_4^{(3-x)-}$ only, $D_{H_xPO_4^{(3-x)-}}$, is also displayed.

FS Anions	**$\Delta[H_xPO_4^{(3-x)-}]$**	**$D_{H_xPO_4^{(3-x)-}}$ (%)**
$H_xPO_4^{(3-x)-}$	28.67	N/A
$H_xPO_4^{(3-x)-}$, SO_4^{2-}	27.1	5.26
$H_xPO_4^{(3-x)-}$, Cl^-	24.7	13.7
$H_xPO_4^{(3-x)-}$, SO_4^{2-}, Cl^-, i.e., fresh urine	23.4	18.0

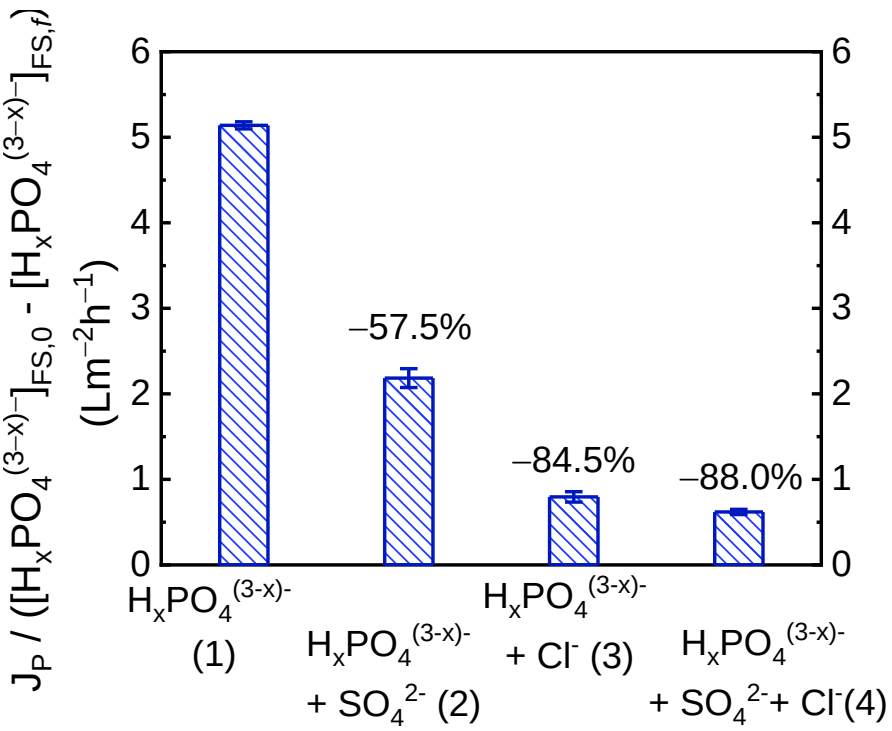

Figure S2. Orthophosphate ion flux, J_P, normalized by $[H_xPO_4^{(3-x)-}]_{FS,0} - [H_xPO_4^{(3-x)-}]_{FS,f}$ in DD kinetic experiments with four FS of 1) 30×10^{-3} mol-$H_xPO_4^{(3-x)-}$/L, 2) 30×10^{-3} mol-$H_xPO_4^{(3-x)-}$/L and 16×10^{-3} mol-SO_4^{2-}/L, 3) 30×10^{-3} mol-$H_xPO_4^{(3-x)-}$/L and 100×10^{-3} 10^{-3} mol-Cl^-/L, and 4) 30×10^{-3} mol-$H_xPO_4^{(3-x)-}$/L, 100×10^{-3} mol-Cl^-/L, and 16×10^{-3} mol-SO_4^{2-}/L. All experiments were operated with V_{FS}/V_{RS} = 1 and 600×10^{-3} mol-NaCl/L as the receiver solution. Data points and error bars are means and standard deviations, respectively, of duplicate experiments. The labels above the columns indicate the change in orthophosphate flux relative to experiments with orthophosphate only feed solution, i.e., FS (1).

SORPTION EXPERIMENT PROTOCOL

AMV membrane coupon of 9.0 cm^2 (0.099 cm^3 volume) was submerged in 50 mL of the feed solution for >24 h to equilibrate. Then, the membrane coupon was transferred to a fresh 50 mL feed solution for another two times for >24 h each, to ensure that previous ion sorption does not interfere with the analysis. Next, the membrane coupon was removed from the feed solution and carefully wiped using a Kimwipe to ensure no residual solution remained on the membrane surface. The membrane coupon was then submerged in 50 mL of DI water for >24 h. After which, the membrane coupon was transferred to 50 mL of 0.10 M $NaNO_3$ rinse solution for >24 h to enable the desorption of ions. The membrane coupon was immersed in another 50 mL of 0.10 M $NaNO_3$ rinse solution for >24 h to complete the ion desorption. Ion chromatography was used to analyze the ion concentrations in the DI water and rinse solutions. The total moles in all three solutions were used to determine the total amount of ions sorbed into the AMV membrane. Sorption coefficient, X, is defined as ions sorbed into the membrane ($\times 10^{-3}$ moles/cm^3 membrane) normalized by molar concentration in the feed solution.

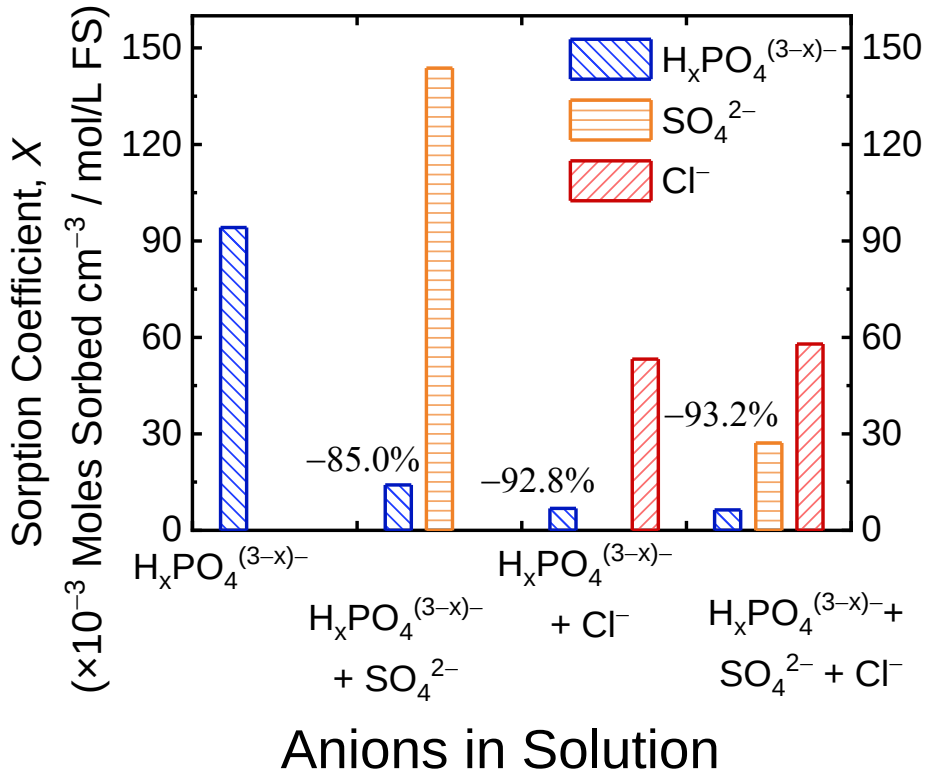

Figure S3. Sorption coefficient, *X*, for orthophosphate, sulfate, and chloride into AMV membrane for FS of: 1) 30×10^{-3} mol-$H_xPO_4^{(3-x)-}$/L, 2) 30×10^{-3} mol-$H_xPO_4^{(3-x)-}$/L and 16×10^{-3} mol-SO_4^{2-}/L, 3) 30×10^{-3} mol- $H_xPO_4^{(3-x)-}$/L and 100×10^{-3} 10^{-3} mol-Cl^-/L, and 4) 30×10^{-3} mol- $H_xPO_4^{(3-x)-}$/L, 100×10^{-3} mol-Cl^-/L, and 16×10^{-3} mol-SO_4^{2-}/L, i.e., fresh urine. Sorption coefficient is defined as ions sorbed into the membrane ($\times10^{-3}$ moles/cm^3 membrane) normalized by molar concentration in the feed solution.

Table S7. Area specific resistance of Selemion AMV and ASVN membranes for different electrolytes (2018).

	Area Specific Resistance ($\Omega\,cm^2$)	
Electrolyte	**AMV**	**ASVN**
0.5 mol/L NaCl	2.8	3.7
0.25 mol/L Na_2SO_4	5.5	13
0.5 mol/L HCl	2.5	3.1
0.25 mol/L H_2SO_4	7.0	9.5

IMPACT FLUX

The high concentration of HCO_3^- ions in hydrolyzed urine greatly suppresses J_P, with reductions of 97.3% and 72.4% in the orthophosphate fluxes relative to TOP-only feed solution and fresh urine, respectively (Figure 6 of the main manuscript). The high HCO_3^- content similarly affects J_S (59.2% lower with hydrolyzed urine than fresh urine). DD with hydrolyzed urine resulted in predominantly HCO_3^- and Cl^- exchange, with J_C > 8× higher than J_P and J_S. As discussed in the preceding paragraph, anions in a multi-component FS compete to sorb into the AEM. In particular, the high concentration of HCO_3^- present in hydrolyzed urine (Udert et al., 2003) is expected to strongly favor the partitioning of bicarbonate anions into the AEM, which in turn hinders the fluxes of other ions. Importantly, $J_C >> J_P$ supports the conjecture discussed in the main manuscript that bicarbonate transport from FS to RS significantly outpaced orthophosphate transport, which resulted in the apparent stagnation of $[H_xPO_4^{(3-x)-}]_{RS,f}$ before Donnan equilibrium was reached in the experiments. Compared to fresh urine as the feed solution, utilizing hydrolyzed urine resulted in lower $[H_xPO_4^{(3-x)-}]_{RS,f}$, less orthophosphate recovery, more significant deviations from the Donnan equilibrium, and reduced J_P (Figures 5 and 6 of the main manuscript). For these reasons, it is more advantageous for DD to target fresh urine for orthophosphate recovery.

REFERENCES

2018 Selemion: Ion Exchange Membranes, ACG Engineering Co., LTD.

2021 PuroLite Product Guide: Product Characteristics and Applications. PuroLite (ed).

Kuda, T. and Yano, T. 2014. Mineral Composition of Seawater Bittern Nigari Products and Their Effects on Changing of Browning and Antioxidant Activity in the Glucose/Lysine Maillard Reaction. Appl Biochem Biotechnol 172, 2989–2997.

Michaud, C.F. 1999a. Factors Affecting the Brine Efficiency of Softeners, Part 1. Water Conditioning & Purification, 36-38.

Michaud, C.F. 1999b. Factors Affecting the Brine Efficiency of Softeners, Part 2. Water Conditioning & Purification, 76-78.

Purolite: Water Softening Basics. https://www.purolite.com/application/softening/How-do-water-softeners-work.

Udert, K.M., Larsen, T.A., Biebow, M. and Gujer, W. 2003a. Urea hydrolysis and precipitation dynamics in a urine-collecting system. Water Res. 37(11), 2571-2582.